Proceedings of the 11th ICPMG 2026
11th International Conference on Physical Modelling in Geotechnics
8-12 June 2026, Zurich, Switzerland

Interpreting CO_2 plume evolution in hypergravity experiments using integrated monitoring data

S. Lopez Saavedra, M. Shafaei Bajestani, R. Chalaturnyk, G. Zambrano Narvaez
University of Alberta, Edmonton, Canada, lopezsaa@ualberta.ca, mshafaei@ualberta.ca, rc11@ualberta.ca, gonzalo@ualberta.ca

ABSTRACT: A major challenge in establishing carbon storage as a viable solution for mitigating greenhouse gas emissions lies in accurately tracking and monitoring the behavior of injected carbon dioxide (CO_2) underground. Laboratory-scale investigations are essential for providing reliable benchmarks to validate numerical models and improve understanding of CO_2 movement in the subsurface. This study analyzes data from hypergravity experiments performed in a geotechnical centrifuge to simulate subsurface carbon sequestration. The objective is to analyze experimental data to track fluid-phase evolution and evaluate field-scale operational diagnostic parameters that characterize CO_2 dynamics. High-resolution imaging was used to track gas-phase development, while multilevel pressure measurements were processed to compute diagnostic gradients indicative of fluid movement during pressure buildups associated to gas injection. Image segmentation shows that the gas cap during the first pressure buildup reached approximately 117 cm², followed by rapid pressure dissipation driven by CO_2 dissolution into the aqueous phase. In the second buildup, the gas cap expanded concavely to cover and area of approximately 130 cm², producing a more gradual pressure response consistent with gas accumulation in a structural trap. Diagnostic vertical pressure gradients captured plume intersection, downward aqueous flow in certain compartments, and upward trends in regions isolated by geological boundaries. These findings demonstrate the potential of centrifuge modeling to provide quantitative data into CO_2 behavior under subsurface conditions and highlight the value of combining high-resolution imaging, pressure diagnostics, and computational tools to better understand CO_2 migration in laboratory-scale subsurface models.

1 INTRODUCTION

The rise in atmospheric carbon dioxide (CO_2) remains a key driver of global warming, motivating the development of technologies that can reduce emissions and stabilize climate trends. Geological CO_2 storage is increasingly recognized as a major long-term mitigation option. However, carbon sequestration projects require reliable methods to predict and verify CO_2 movement underground.

Predicting CO_2 behavior is challenging because of the limited knowledge of subsurface conditions. Monitoring tools can track injected CO_2, but they are not always available, making numerical simulation essential in project planning and assessment.

Validating simulation results for CO_2 storage is inherently difficult due to the lack of controlled, field datasets. Benchmarking exercises provide a structured approach to evaluate simulation performance by comparing models against reference cases (Oberkampf and Trucano, 2008). FluidFlower benchmarks have gained widespread adoption for simulations of CO_2 injection under well-defined conditions (Eikehaug et al., 2024; Fernø et al., 2024; Haugen et al., 2024; Nordbotten et al., 2022).

One promising approach for generating experimental datasets for CO_2 sequestration research is to conduct laboratory experiments at elevated pressures, enabling more realistic subsurface conditions. Centrifuge modeling can recreate an environment in which the porous media experience increased pore pressures and stress levels.

Pressure data are essential for validating numerical simulations (Bourne et al., 2014). Pore pressure measurements help determine whether CO_2 remains within intended compartments and provide information about injection and post-injection monitoring (Chadwick et al., 2009). These data also assist in evaluating the influence of internal barriers and heterogeneities and identify monitoring signals most indicative of plume movement (Strandli and Benson, 2013).

This paper examines data from a hypergravity test conducted in a geotechnical centrifuge that investigated CO_2 sequestration under pressure gradients and stress conditions. The objective is to process the experimental dataset to track fluid-phase evolution over time and assess field-scale diagnostic indicators that describe CO_2 movement. The approach integrates image analysis for monitoring fluid-phase behavior with pressure-based diagnostic gradients used to evaluate plume dynamics. These efforts contribute toward developing a computational platform for processing data from future centrifuge-based supercritical CO_2 storage experiments.

2 METHODOLOGY

2.1 Experimental dataset from centrifuge modeling

The dataset analyzed in this work was generated at the Geotechnical Centrifuge Experimental Research Facility (GeoCERF) at the University of Alberta (Figure 1), which operates a 2-m radius beam centrifuge capable of generating up to 150 g (Zambrano-Narvaez and Chalaturnyk, 2014).

The experiment consisted of a CO_2 storage test conducted in the centrifuge using a plane-strain strongbox of 800 × 450 × 387 mm in size. Inside, a porous-media specimen measuring approximately 289 mm × 1 cm × 656 mm, was constructed by depositing soil materials (sand and clay) with varying properties to represent a subsurface geological reservoir anticline with an overlying seal rock and a repeated geological sequence. To construct the model geometry, the design was first sketched on the metal back plate, after which the porous media material was deposited using a pluviator device through the 1 cm gap. For the clay, small spherical portions were placed into the gap and then compacted with laboratory tools.

The test procedure involved first saturating the specimen with distilled water for 24 hours. Afterward, the centrifuge was spun at 100 g for 30 minutes to overconsolidate the model and prevent seal fracturing during the subsequent CO_2 injection test at 50 g. Afterward, the sample was saturated with a pH indicator solution for 24 hours to enable visualization of CO_2 displacement. Finally, CO_2 was injected to the sample while centrifuge was spinning, and the sample is saturated with the pH indicator solution. Carbon dioxide displacement was monitored through pore-pressure sensors and a visualization system that tracks color changes in the pH indicator resulting from fluid reactions. The pH-sensitive solution was initially green and, upon contact with CO_2 gas, gradually changed to its color indicating an increase in acidity, CO_2 dissolution, or an increase in CO_2 concentration.

Figure 1. GeoCERF Geotechnical Centrifuge.

The experiment measured pressure at multiple reservoir compartments at different locations across the porous media (Figure 2) during the CO_2 injection test. The sensors were labeled according to their horizontal position within the sample, left (L), middle (M), and right (R), and with respect to their elevation, with the lowest-elevation sensors numbered from 1 at the bottom to 4 at the top. Further details are available in a separate source (Lopez-Saavedra et al., 2025).

This paper focused on analyzing the images and pressure data collected during two pressure buildups (PBUs) from this experiment. PBUs were selected because the gas-phase signature can be clearly distinguished in both the images and the pressure responses. Dissipation of the gas cap due to CO_2 dissolution is visible in the images and in the pressure response because of the relatively large gas volume. However, smaller-scale dissolution events may require more advanced processing to interpret reliably from pressure data. From the original dataset, the monitoring sensors analyzed in this study (Table 1), were chosen to provide coverage across the left, middle, and right sides of the sample, as well as across different compartments. The injection location was not included because this data is influenced by injection pressure and therefore do not represent an independent plume-monitoring site.

Table 1. Pressure sensors analyzed.

Sensor analyzed	Location in the sample	Reservoir compartment
L_1, L_2	Left column	RC_1
L_3	Left column	RC_4
M_2, M_3	Middle column	RC_1
R_1, R_2	Right column	RC_2
R_3	Right column	RC_3

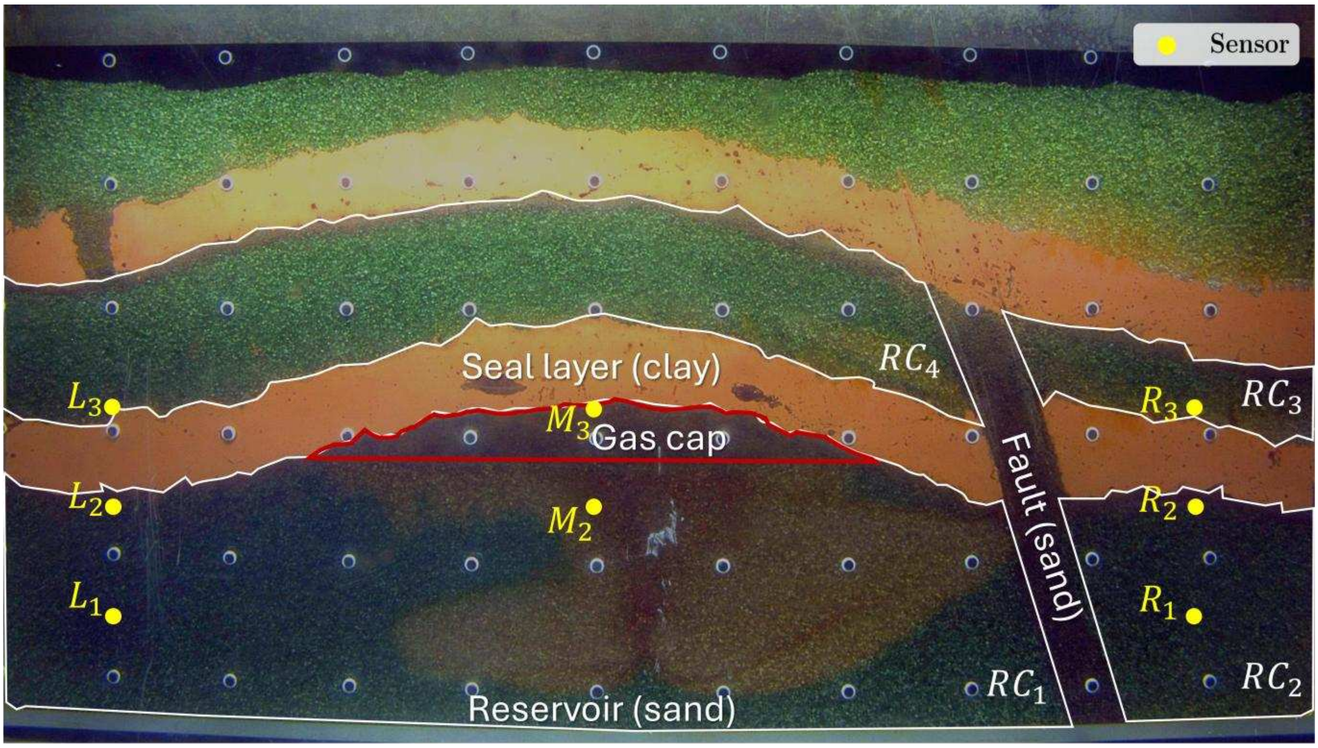

Figure 2. Sample showing sensor locations, compartments, soil types, and gas-cap identified by pH indicator color.

2.2 Image analysis

To quantify regions of maximum gas saturation (mobile or immobile gas), we assumed that the pressure buildups indicated zones of maximum gas saturation (i.e., minimal aqueous-phase saturation). Based on this assumption, image segmentation of the aqueous and gaseous phases was performed in Python for each pressure-buildup image considering that the gas-cap area was defined as the region with the strongest red tone. Further details on analyzing fluid reactions of the pH-sensitive solution in contact with CO2 are provided elsewhere (Haugen et al., 2024; Nordbotten et al., 2024).

Pressure data were matched to images using the elapsed time between logs. The sample domain measured approximately 65.3 cm × 28.9 cm (≈37.7 cm including a free water level), corresponding to an image resolution of 2048 × 1162 pixels.

The physical area per pixel, A_{pixel} (cm/pixel) was computed by multiplying the pixel-normalized width W_{px} (cm/pixel) by the pixel-normalized height H_{px} (cm/pixel):

$$A_{pixel} = W_{px} \times H_{px} \qquad (1)$$

The gas area A_{gas} (cm^2) was then obtained by multiplying the number of gas pixels identified through image segmentation (Figure 2) by A_{pixel}:

$$A_{gas} = (\#\, gas\, pixels) \times A_{pixel} \qquad (2)$$

2.3 Pressure buildups

The differential pressure buildup for each sensor as a function of time is defined as:

$$\Delta P_s = P_s(t) - P_{s,init} \qquad (3)$$

Where $P_s(t)$ (kPa) is the pressure at time t, and $P_{s,init}$ (kPa) is the initial pressure for sensor s.

2.4 Vertical pressure gradients

The normalized vertical pressure gradient (Strandli and Benson, 2013) is given by:

$$\left(\frac{\Delta P_{\Delta z}(t)}{\Delta P_{\Delta z,init}}\right)_{j,i} = \frac{P_j(t) - P_i(t)}{P_{j,init} - P_{i,init}} \qquad (4)$$

Where sensors j and i are vertically aligned, with j located below i. A normalized vertical pressure gradient ratio near unity indicates no vertical flow when the plume does not intersect the monitoring location; if the CO_2 plume intersects the sensor, the ratio decreases due to the lower density of CO_2 relative to water. A ratio of more than 1 points to upward flow; and a ratio below 1 indicates downward flow (Figure 3).

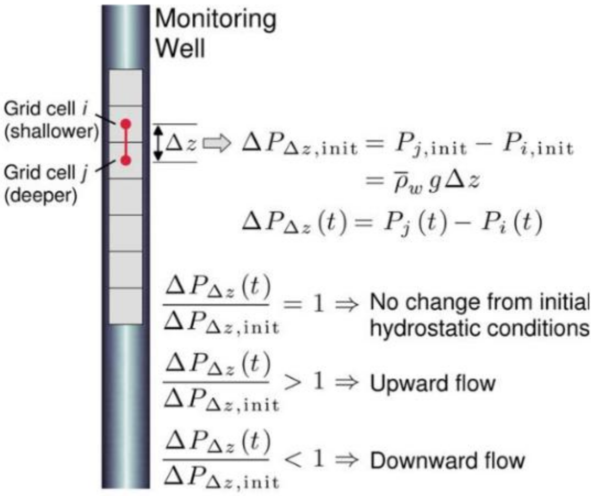

Figure 3. Equation 4 is used to calculate the normalized vertical pressure gradients between vertically aligned sensors (Strandli and Benson, 2013).

3 RESULTS AND DISCUSSIONS

3.1 Gas-phase plumes

Analysis of images from the two pressure buildups shows that in centrifuge-based CO_2 sequestration experiments, regions of maximum gas saturation can be identified through image analysis alone, thanks to the tonalities of the pH-sensitive solution. However, integrating pressure data improves the precision of gas-plume delineation and its growth pattern, and aids in timing its dissolution in the aqueous phase.

During the first pressure buildup, the gas cap reached approximately 117 cm^2 (Figure 4a) shortly after gas entered the sample (Figure 4b). The differential pressure at sensor M_3 peaked at approximately 38 kPa, followed by rapid convex dissipation to around 20 kPa, and then a slower decline as CO_2 dissolved into the aqueous phase (Figure 4c). The evolution of the gas cap area and the associated pressure response are consistent with rapid initial CO_2 dissolution, followed by progressively slower mass transfer as equilibrium is approached (Tayeb et al., 2023). On the other hand, although the gas-cap area trend is clear, enhancing the precision of the image segmentation method may help smooth the transitions between consecutive data points.

In the second buildup, the gas cap expanded concavely to approximately 130 cm^2 (Figure 5a), corresponding to gas saturating the anticline structure beneath the seal (Figure 5b). The differential pressure at M_3 increased concavely to approximately 25 kPa, followed by gradual concave dissipation to near 12 kPa (Figure 5c), consistent with dissolution-driven reduction in gas-phase volume. Similar to the first buildup, the trend in the gas-cap area is clear, but the transitions between subsequent data points should be smoother, which could be achieved by improving the image segmentation process.

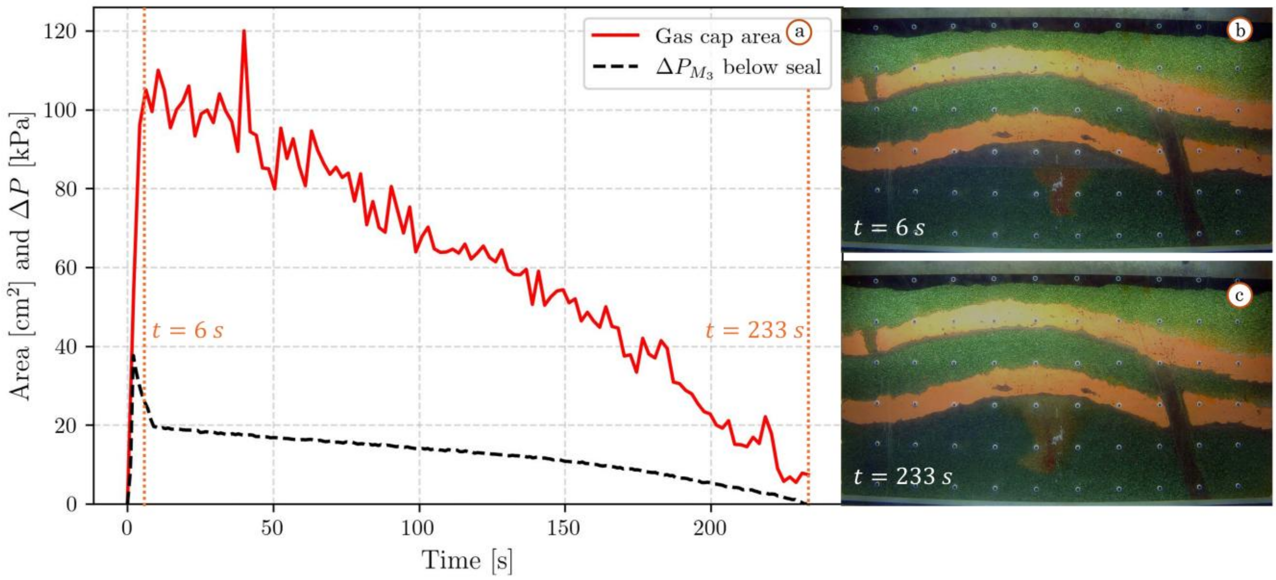

Figure 4. (a) Estimated gas cap area during PBU1 obtained through image processing. (b) Gas cap associated with gas breakthrough at t = 6 s. (c) Dissipation of gas cap due to dissolution in the aqueous solution at t = 233 s.

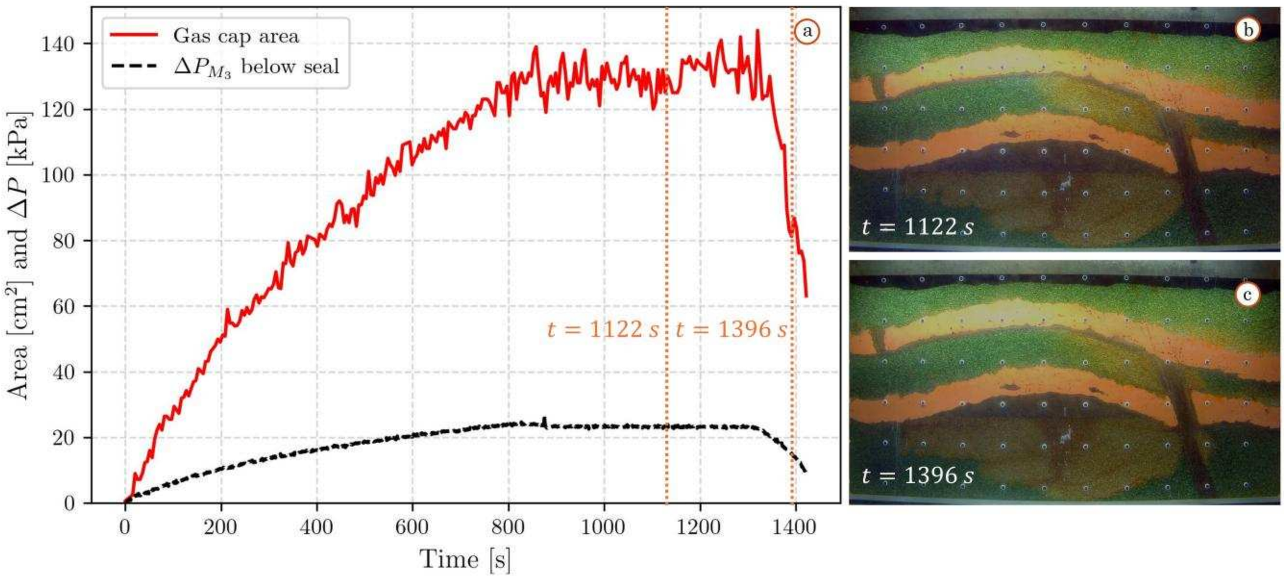

Figure 5. (a) Estimated gas cap area during PBU2 obtained through image processing. (b) Gas cap area associated with gas accumulation at t = 1122 s. (c) Dissipation of gas cap due to dissolution in the aqueous solution at t = 1396 s.

3.2 Diagnostics for CO_2 migration

For PBU1, the normalized vertical pressure gradient ratio, M_2, M_3, drops sharply from 1 to near 0.25 early in the buildup, indicating CO_2 plume intersection at this location (Figure 6a). On the left side of the sample, both L_1, L_2 and L_2, L_3 show trends below unity after an initial spike, indicating downward aqueous flow (Figure 6b). In turn, the average values for these parameters over the zoomed range are below unity (Figure 6b and Figure 7a).

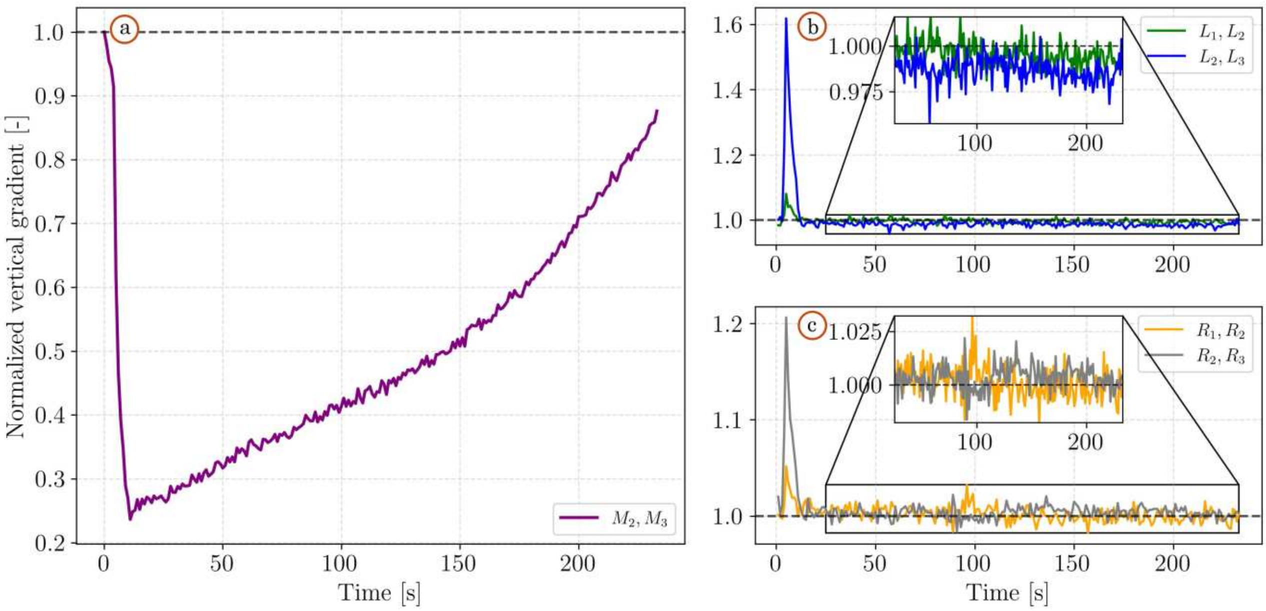

Figure 6. Normalized vertical pressure gradient calculations for PBU1. (a) Middle ratio (M_2, M_3) shows a sharp drop due to the gas entry into the sample. (b)After gas breakthrough, the left-side monitoring ratios (L_1, L_2 and L_2, L_3) shows trends below unity which suggest downward flow of the aqueous phase. (c) The right-side monitoring ratios (R_1, R_2 and R_2, R_3) exhibit near-hydrostatic behavior, likely due to the present fault limiting pressure communication.

These trends align with image-based observations showing dissolution-driven plume reduction. On the right-side, R_1, R_2 and R_2, R_3 exhibit near-hydrostatic behavior, likely due to the geological fault restricting lateral pressure communication (Figure 6c and Figure 7a).

For PBU2, M_2, M_3 exhibits an initial sharp drop from near 0.9 to approximately 0.05, indicating gas-cap growth, followed by a plateau that suggests the gas cap has stopped growing, and then an upward trend as aqueous flow becomes more dominant (Figure 8a). On the left side, L_1, L_2 remains below unity, indicating downward flow, whereas L_2, L_3 shows a hydrostatic trend until the end of the dataset, where it starts to go downwards (Figure 8b). The average value for L_1, L_2 over this range is below unity, whereas the average for L_2, L_3 is near one (Figure 7b). On the right side, R_1, R_2 remains below unity, indicating downward aqueous flow, while R_2, R_3 stays above unity suggesting upward flow, indicating local compartmentalized behavior (Figure 8c and Figure 7b).

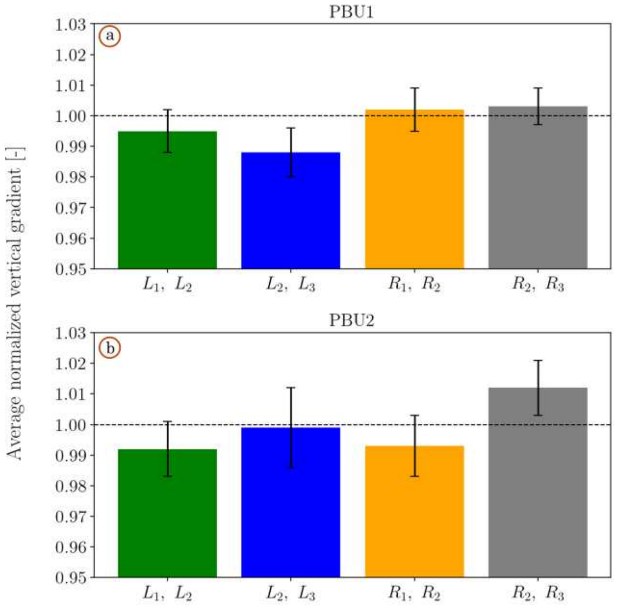

Figure 7. Average normalized vertical gradient for (a) PBU1 and (b) PBU2.

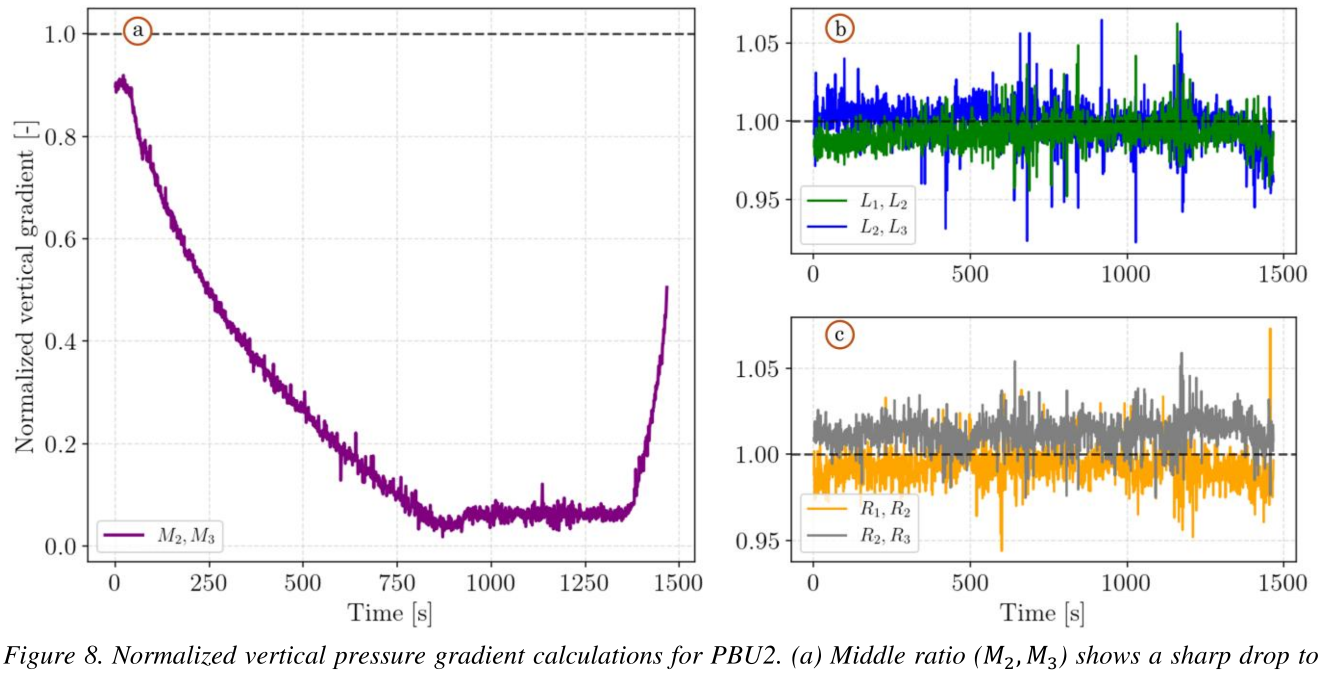

Figure 8. Normalized vertical pressure gradient calculations for PBU2. (a) Middle ratio (M_2, M_3) shows a sharp drop to the gas presence. (b) The left-side ratio of L_1, L_2 indicates downward flow of the aqueous phase while the L_2, L_3 shows no clear trend until the end of the dataset which shows a decreasing trend. (c) The right-side monitoring ratio of R_1, R_2 indicates downward flow while the ratio of R_2, R_3 indicates upward flow, potentially due to local compartmentalization.

4 CONCLUSIONS

This study reveals the value of combining image analysis and pressure-derived diagnostics to interpret CO_2 plume development in centrifuge-based storage experiments. Image segmentation quantified gas-phase growth across two pressure buildups, revealing distinct behaviors: the first one showed an early, rapid saturation and dissolution-dominated response. The second one showed a slower incremental response structurally controlled by accumulation. Pressure measurements captured these processes through characteristic dissipation curves and diagnostic vertical gradients, which distinguished plume intersection, downward aqueous flow, and regions of limited pressure communication.

These results demonstrate that hypergravity testing can recreate carbon storage subsurface processes, including dissolution dynamics, trap filling, and compartmentalization. The workflow developed here offers an integrated approach for analyzing data from future centrifuge experiments and advances the development of an experimental framework that provides benchmark datasets for numerical simulators.

ACKNOWLEDGEMENTS

The authors gratefully acknowledge the support of Natural Sciences and Engineering Research Council of Canada (NSERC) to the Geoscience for Subsurface Assurance of Energy Technology (GeoSAFETY) program.

REFERENCES

Bourne, S., Crouch, S., Smith, M., 2014. A risk-based framework for measurement, monitoring and verification of the Quest CCS Project, Alberta, Canada. *International Journal of Greenhouse Gas Control* 26, 109–126. https://doi.org/https://doi.org/10.1016/j.ijggc.2014.04.026

Chadwick, R.A., Arts, R., Bentham, M., Eiken, O., Holloway, S., Kirby, G.A., Pearce, J.M., Williamson, J.P., Zweigel, P., 2009. Review of monitoring issues and technologies associated with the long-term underground storage of carbon dioxide. *Underground Gas Storage: Worldwide Experiences and Future Development in the UK and Europe*. D. J. Evans and Chadwick, R. A. (eds.). Geological Society, London, Special Publications 313, 257–275. https://doi.org/https://doi.org/10.1144/SP313.15

Eikehaug, K., Haugen, M., Folkvord, O., Benali, B., Bang Larsen, E., Tinkova, A., Rotevatn, A., Nordbotten, J.M., Fernø, M.A., 2024. Engineering Meter-scale Porous Media Flow Experiments for Quantitative Studies of Geological Carbon Sequestration. *Transp. Porous Media* 151, 1143–1167. https://doi.org/https://doi.org/10.1007/s11242-023-02025-0

Fernø, M.A., Haugen, M., Eikehaug, K., Folkvord, O., Benali, B., Both, J.W., Storvik, E., Nixon, C.W., Gawthrope, R.L., Nordbotten, J.M., 2024. Room-Scale CO2 Injections in a Physical Reservoir Model with Faults. *Transp Porous Media* 151, 913–937. https://doi.org/https://doi.org/10.1007/s11242-023-02013-4

Haugen, M., Saló-Salgado, L., Eikehaug, K., Benali, B., Both, J.W., Storvik, E., Folkvord, O., Juanes, R., Nordbotten, J.M., Fernø, M.A., 2024. Physical Variability in Meter-Scale Laboratory CO2 Injections in Faulted Geometries. *Transp Porous Media* 151, 1169–1197. https://doi.org/https://doi.org/10.1007/s11242-023-02047-8

Lopez-Saavedra, S., Bajestani, M.S., Pantov, D., Chalaturnyk, R., Zambrano-Narvaez, G., 2025. Hypergravity experiments on meter-scale porous media flow for geological carbon sequestration. *Sci. Rep.* 15, 45712. https://doi.org/10.1038/s41598-025-28226-9

Nordbotten, J.M., Benali, B., Both, J.W., Brattekås, B., Storvik, E., Fernø, M.A., 2024. DarSIA: An Open-Source Python Toolbox for Two-Scale Image Processing of Dynamics in Porous Media, *Transport in Porous Media*. Springer Netherlands. https://doi.org/https://doi.org/10.1007/s11242-023-02000-9

Nordbotten, J.M., Fernø, M., Flemisch, B., Juanes, R., Jørgensen, M., 2022. Final Benchmark Description: FluidFlower International Benchmark Study. https://doi.org/https://doi.org/10.5281/zenodo.6807102

Oberkampf, W.L., Trucano, T.G., 2008. Verification and validation benchmarks. *Nuclear Engineering and Design* 238, 716–743. https://doi.org/https://doi.org/10.1016/j.nucengdes.2007.02.032

Strandli, C.W., Benson, S.M., 2013. Identifying diagnostics for reservoir structure and CO2 plume migration from multilevel pressure measurements. *Water Resour Res* 49, 3462–3475. https://doi.org/https://doi.org/10.1002/wrcr.20285

Tayeb, F., Rouabhi, A., AbuAisha, M., Valtz, A., 2023. Kinetics of CO2 dissolution for underground applications. *Geoenergy Science and Engineering* 230, 212061. https://doi.org/https://doi.org/10.1016/j.geoen.2023.212061

Zambrano-Narvaez, G., Chalaturnyk, R.J., 2014. The New GeoREF Geotechnical Beam Centrifuge at the University of Alberta, Canada. *Physical Modelling in Geotechnics - Proceedings of the 8th International Conference on Physical Modelling in Geotechnics 2014*, ICPMG 2014 1, 163–167. https://doi.org/https://doi.org/10.1201/b16200-15